Available online at www.sciencedirect.com
SCIENCE DIRECT
Journal of Colloid and Interface Science 300 (2006) 735–743
JOURNAL OF Colloid and Interface Science
www.elsevier.com/locate/jcis

Bubble motion measurements during foam drainage and coarsening

G. Maurdev, A. Saint-Jalmes *, D. Langevin

Laboratoire de Physique des Solides, Université Paris-Sud, 91405 Orsay Cedex, France

Received 28 November 2005; accepted 31 March 2006
Available online 4 May 2006

Abstract

We have studied bubble motion within a column of foam allowed to undergo free drainage. We have measured bubble motion upward with time and as a function of their initial positions. Depending on the gas used, which sets the coarsening and drainage rates, different bubble upward motion types have been identified (constant speed, acceleration or deceleration) and explained in relation with liquid downward flows. The proofs of the consistency between bubble upward motion and liquid downward flow are obtained both by comparing the bubble motion curves to the liquid drainage ones, and by comparing the time variations of the liquid fraction extracted from bubble motion to direct liquid fraction measurements by electrical conductimetry. The agreement between bubble position tracking and electrical conductivity shows in particular that it is possible to determine the drainage regime from such simple bubble motion measurements. This work also allowed us to demonstrate a special case of foam coarsening and expansion, occurring when the foam gas is less soluble than the outside one, caused by diffusion of this external gas into the foam. All these results allow us to build a picture of drainage and coarsening seen from the bubble point of view.

Keywords: Foams; Drainage; Coarsening; Bubble

1. Introduction

Aqueous foams are unstable systems: they irreversibly evolve with time, via drainage and coarsening processes [1,2]. Due to gravity, a foam drains: the liquid initially distributed between the bubble flows down, and the foam liquid fraction, $\varepsilon = V_{\text{liquid}}/V_{\text{foam}}$ always decreases (V_{liquid} is the volume of liquid dispersed inside a foam of volume V_{foam}). The liquid flows in a randomly oriented network of interstitial channels, the Plateau borders (PBs), with scalloped-triangular sections depending on the liquid fraction ε. Foam drainage shares some features with the propagation of liquid into porous media, but with the specificity that the pore size (the PB section for foams) is dynamically coupled to the amount of liquid, and that these PB walls are viscoelastic gas–liquid interfaces. With time, a foam also coarsens, the mean bubble size increases, as a result of gas diffusion from bubbles with small number of faces (with greater Laplace pressure) to bubbles with a larger number of faces (with smaller internal pressure) [1–3]. Finally bubble size can grow as thin films between adjacent bubbles rupture, resulting in bubble coalescence.

In the recent years, much progress has been made in understanding foam drainage kinetics [4–15]. Different flow regimes have been reported, corresponding to different interfacial surface mobilities [10–15]. This interfacial mobility (incorporating the bubble size, the interfacial and bulk viscoelastic properties and the liquid fraction) describes the coupling between flow inside the PBs and at their surfaces. Experimentally, measurements are usually made at macroscopic scales (one measures for instance the speed or width of a drainage front, or the volume of drained liquid with time). The techniques used, even local ones like electrical conductivity [1,2,16] or light scattering [5,8], allow us to scan time evolution on large scales (typically centimeters, when bubbles are less than millimeters). In that sense, it is then often stated that the foam is described at an effective-medium level, with a continuous liquid fraction with height, not considering any fine structural detail. Such assumptions, used in most models, are validated by agreement between models and macroscopic observation. In these theoretical approaches, the macroscopic behavior is directly derived from the microscopic description of the flow inside a single PB.

* Corresponding author.
E-mail address: saint-jalmes@lps.u-psud.fr (A. Saint-Jalmes).

0021-9797/$ – see front matter
doi:10.1016/j.jcis.2006.03.079

Recently, experiments focusing at this scale of a single PB also confirm the theoretical description and agree with macroscopic measurements (for instance, for the estimation of surface shear viscosities) [12–14], giving support to theories at both macroscopic and PB length scales.

However, one can consider if different descriptions of drainage could be given, and for instance at the intermediate scale of the bubble size. As a foam freely drains, the liquid flows down and accumulates at the bottom of the sample container. At the same time, it is clear that the foam height is changing and that the bubbles are rising. It is then interesting to know the dynamics of the bubble motion, and how drainage is seen from the point of view of a bubble (depending also on the initial vertical position of that bubble). Indeed, it is also important to test if the upward bubble motion is always consistent with the downward liquid flow, whatever the experimental conditions, and with the possible coupling with coarsening [8,17,18], and if one can infer information about drainage and foam aging by simply monitoring bubble rise. Finally, one can also note that experimental methods usually provide measurement at a fixed position in the cell, and assume a constant foam height and an immobile PB skeleton: in the simple situation of free drainage, as the bubble move upward, the measurements are not always done on the same bubbles, and one may thus ask about the impact it may have on the measurements.

In this paper, we address the issue of bubble rise in a foam undergoing free drainage. We present a simple technique providing us with a measurement of the bubble motion during drainage, for any initial height in the foam. Both bubble motion results obtained for different combinations of inside/outside gas (allowing coarsening or not, as drainage proceeds), and liquid fraction variations (given by electrical conductivity measurements) are reported. This allows us to demonstrate different types of dynamics, to show that we can recover information on the drainage by simply following the bubble motion, and to check the consistency between upward bubble motion and macroscopic downward liquid drainage features.

2. Experimental conditions, setup and definitions

Experiments are performed with foams made by the turbulent mixing method [5]. A high pressure jet of gas and liquid are mixed within a small diameter tube. The mean bubble diameter D is 100 μm, with low polydispersity (no bubbles with diameters twice bigger or half smaller than the mean value, and relative deviation of 0.2) [5]. With that technique, the initial liquid fraction ε_0 can be selected from 0.03 to 0.5 by monitoring the gas and liquid flow rates. This method has the advantage of producing liters of foam in a few seconds: it is then possible to fill our transparent Plexiglas measurement cell (height $h_c = 500$ mm, width $w = 125$ mm, thickness $t = 25$ mm) with a perfectly uniform foam in 15–20 s (depending on the liquid fraction). Practically, we only filled up to $h_0 \approx 400$ mm, to leave space available for foam expansion. We used aqueous solutions of sodium dodecyl sulfate (SDS) (at concentration $c = 6$ g/L), and two different gases, nitrogen (N_2) and perfluoroethane (C_2F_6). The coarsening rate depends on the solubility and diffusivity of the gas into the liquid [17]: with C_2F_6, one obtains a coarsening rate 30 times smaller than with N_2 (for given initial bubble diameter and liquid fraction [17]). With the latter, for $D < 1$ mm and for foam column of at least 20 cm high, a significant coarsening (D varies by a factor 10) during drainage can be observed [8,17].

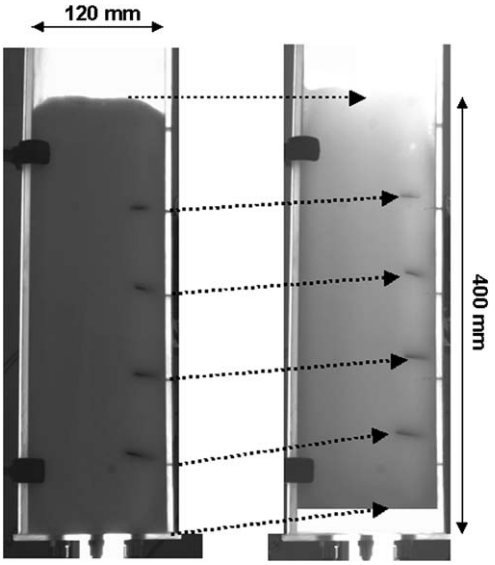

Fig. 1. Pictures of the foam, illuminated form the back, at $t = 1000$ s and $t = 6000$ s after foam formation. Case of a foam made with C_2F_6, in contact with the same gas. The arrows indicate the motion of the markers, of the liquid-foam interface and of the foam top. As the foam drains, it appears brighter in transmission.

To investigate the way in which the bubbles in a draining foam rearrange, a simple technique was devised where small pieces of dark flat card (1.4×1.4 cm^2) are inserted via small slits cut into the side of the column. These markers, inserted at vertical position z_0, rest in flat positions, and do not come in contact with the walls. They can however still be seen from the outside (Fig. 1). As they are very light, they are trapped within the structure of the foam: when the bubbles move, they also moved along with them. In Fig. 1, two pictures of the foam, illuminated from the back, are shown (at times t after foam formation: $t = 1000$ s on the left, and $t = 6000$ s on the right). One can see the upward displacement of all the markers and of the foam–liquid interface, as indicated by the arrows. As well, one can see the increase of transmitted light through the foam, showing that the foam has drained and that the liquid fraction has decreased [8]. Note also that the markers are only located on a small part of the foam section, and that we have not detected any local effects due to them, when compared to the rest of the foam. The marker vertical displacement, $L(t) = z(t) - z_0$, is monitored as a function of time via a CCD camera, and a light intensity analysis of a vertical section of the foam allows the precise position of each marker to be monitored with an accuracy of ± 0.5 mm. Positions of the foam–liquid interface at the bottom and of the foam top are monitored without the help of markers. A limit of this marker tracking technique is that only low initial liquid fraction ε_0 can be studied ($\varepsilon_0 < 0.1$); for

higher ε, the foam is not stiff enough to trap the markers between bubbles.

We have also monitored the foam free drainage features by electrical conductivity measurements. The conductance C of a foam increases with the liquid fraction, and a calibration curve valid in the whole range of liquid fraction (from 0 to 100%) has recently been proposed [16]. Measurements are made in a cell with the same dimensions and foam composition to the ones studied for bubble motion; details of our apparatus can also be found in [16]. The conductivity measurement is local in the sense that it is at a fixed height, over a typical elementary volume V_e (corresponding to a foam height typically equal to the cell thickness, here 2.5 cm). Such V_e spans over many bubbles, and thus the foam is considered as an effective continuous medium, where the bubble structure and more so their motion is not taken into account.

3. Theoretical background

In this section, we first recall recent observations and predictions for the free drainage case (meaning a foam, initially uniform and homogeneous, at liquid fraction ε_0, simply draining at rest). As already stated, depending on the interfacial mobility, describing the coupling between the bulk flow and the interfacial one in the Plateau borders (PBs), different drainage regimes can be found [10–15]. In a large range of experimental conditions, this interfacial mobility is set by the dimensionless parameter $M = \frac{\mu r}{\mu_s}$, where μ is the bulk shear viscosity, μ_s the surface shear viscosity and r the radius of curvature of the PBs [10–14]. When there is no coupling between bulk and surface flow, the PBs surfaces are immobile, and the main hydrodynamic resistance to the liquid flow is within the PBs. Oppositely, for strong coupling, the main contribution to resistance comes from the flow in the nodes, as the viscous dissipation inside the PBs has vanished due the occurrence of flow within their surfaces.

Macroscopically, different behavior are found whether the foam mobility is high or low: for instance, during free drainage, and without coarsening (constant bubble size), one can show that at a given vertical position z', $\varepsilon(t)_{z'} \sim t^{-a}$, with $a = 1$ for low mobility, and $a = 2$ for high mobility [6,8]; such different behaviors were observed by changing the mobility, either via different surfactant or different bubble size [6,8]. Also, the dependence of the height of liquid drained with time, $l(t)$, changes with the drainage regime. One observes, in agreement with predictions, a linear dependence for $l(t)$:

$$l(t) = \beta V_0 l_{\text{int}} t / h_0 \quad \text{for } t \leqslant t_d = h_0/V_0, \tag{1}$$

with $\beta = 1/2$ in the limit of immobile interfaces and $2/3$ for mobile ones; l_{int} is the final height of liquid obtained at the end of the drainage process, and h_0 is the initial height of the foam. The velocity V_0 is defined as

$$V_0 = K_i \frac{\rho g D^2}{\mu} \varepsilon^i, \tag{2}$$

where g is the acceleration of gravity, ρ the solution density, $i = 1$ for low surface mobility and $i = 1/2$ for high surface mobility. The permeability values K_1 and $K_{1/2}$ are dimensionless numbers, depending on the shape of the borders and nodes, but also depending on the interfacial mobility [10–14]. At $t = t_d$, meaning $l/l_{\text{int}} = 1/2$ or $2/3$ depending again on the drainage regime, the linear part of the $l(t)$ curve ends, and an asymptotic behavior is then found as l tends toward l_{int} [5].

When coarsening is significant during drainage, meaning that the typical coarsening time t_c (which depends on the liquid fraction, gas and thin film properties [17,18]) is smaller than the drainage time t_d, it is also known that a coupling between the two effects occurs [8,17,18]. This provides an acceleration of the drainage process, and drainage times which can be divided by 10. In the limit where $t_c \ll t_d$, one can even get a regime where the drainage dynamics is controlled by the coarsening one, in which one finds for instance a quadratic behavior of $l(t)$ at short times ($t \leqslant t_d$).

In these descriptions of free drainage, one considers that all the liquid can eventually leak out of the foam, and that capillary effects are neglected. In a real situation, capillarity effects are also present, tending to bring liquid from wet parts of the foam to drier ones. In fact, taking into account capillarity does not modify the predictions given above (for $\varepsilon(t)$ or $l(t)$) as long as one only considers the steady-state part of the drainage dynamics (at intermediate times) [5–7]. Capillarity, by creating a non-zero equilibrium vertical gradient of ε [1,2,4], is becoming important at long times when this final equilibrium is approached, and especially close to the bottom foam–liquid interface. As a result of this equilibrium vertical profile of ε, there must be layer of high ε at the interface between a foam and its drained liquid, spreading over a capillary length ξ (γ is the liquid surface tension, and we recall that ρ is the surfactant solution density):

$$\xi = \gamma/\rho g D. \tag{3}$$

At the interface, the first bubble layer of the foam is sitting with non-deformed shapes, so that $\varepsilon_c = 0.36$, and the liquid fraction varies from 0.36 to 0.18 over the length ξ [1,2]. However, one must note first that if the foam sample is high enough (as it is the case in these experiments, where $h_0 = 400$ mm), the amount of liquid remaining in this wet foam layer (or capillary hold-up), which is independent of the initial foam height, can become much smaller than the amount of liquid drained, proportional to the foam height. In that case, $l_{\text{int}} \gg \xi$, so that the capillary hold-up effects at the bottom can be neglected. Moreover, if one considers bubbles located at a foam height bigger than a few times ξ, the local equilibrium values of ε is almost zero, and the vertical liquid fraction gradient vanishes, so that capillary effects can also be neglected. Nevertheless, we must also point out that an important consequence of the equilibrium profile at the foam–liquid interface, is that no liquid can actually leak out of the foam before the foam is sufficiently wet (reaching ε_c) at the interface to overcome capillary pressure in the foam [5,8,17].

Regarding the bubble motion, there are boundary conditions imposed by the setup and the free drainage process, which gives us some natural limits for the maximum bubble displacement. Let us consider the simple case of free drainage without coarsening, in a closed reservoir. Free drainage corresponds to a

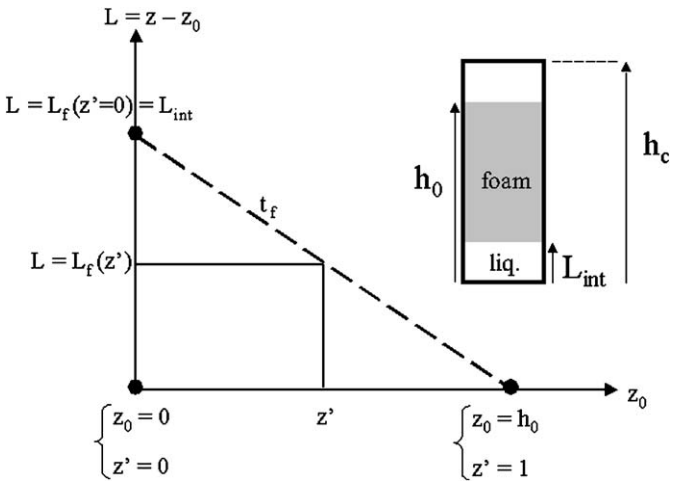

Fig. 2. Diagram summarizing different definitions. For a bubble initially located at z_0 or $z' = z_0/h_0$, the bubble displacement is $L(t) = z(t) - z_0$. At the final time t_f, when no more bubble motion are detected, a bubble reaches its final displacement $L_f(z')$, and the dotted line represents the prediction for this final displacement L_f as a function of the normalized z'. L_{int} is the final position of the foam–liquid interface. The container height h_c is 500 mm, and the initial foam height h_0 is 400 mm.

separation (or a redistribution) process of gas and liquid: as the liquid accumulates at the closed cell bottom, a bubble initially located at that bottom of the foam ($z_0 = 0$), can only move with the foam/liquid interface, always floating on top of the drained liquid. It rises up to a final position $L_f(z_0 = 0) = L_{int}$ (which is the same as l_{int}), and with $L_{int}/h_0 = \varepsilon_0$ (definitions and notations are summarized in Fig. 2). On the contrary, and still considering only the effect of drainage, a bubble initially located at the top, $z_0 = h_0$ (or in normalized units, $z' = z_0/h_0 = 1$), is not expected to move as no liquid is draining from above. If the foam is initially uniform in liquid fraction, and considering both that the bubble motion solely depends on the liquid one, and that the gas and liquid volume are conserved, it is straightforward that, at the end of the drainage process $t = t_f$, the maximum displacement $L_f(z')$ of bubbles initially located at z' $(0 < z' < 1)$ should decrease linearly with z', from L_f $(z' = 0) = L_{int}$ to $L_f(z' = 1) = 0$, as illustrated by the dotted line in Fig. 2. If one considers now a foam undergoing only coarsening (at a constant liquid fraction) and assuming no gas leaks from the foam to the outside its volume should increase as a result of the mean bubble size growth and decrease of the average Laplace pressure P inside the foam bubbles. Quantitatively, for a bubble diameter rising from 100 μm to 2 mm, the change in absolute pressure inside the bubbles remains quite small, $\delta = \Delta P/P \sim 1\%$, and such coarsening can finally only provide an expansion in volume of 1% of the initial volume. But, for a coarsening foam open to the outside, as the Laplace pressure in the bubbles is always higher than the outside pressure, the foam may also loose its gas with time, resulting in a foam height decrease. Here again, quantitatively, as the difference of pressure inside the bubble and outside is small compared to this outside pressure ($\delta \ll 1$), the rate and amount of gas leaking out of the foam are small. Thus, it appears that the coarsening process cannot provide large bubble motion, at least as large of the ones obtained by drainage, as the possible displacement are always proportional to δ (if one does not consider film rupturing, and the extreme case at very long times, where the number of bubbles is so small, that only a few large bubbles remain in the cell). Nevertheless, regarding our setup (closed reservoir at the bottom) a bubble at $z' = 0$ cannot move in response to coarsening, and the bubbles at the top must have the maximum of upward (or downward) motion, as all the foam volume changes can only be in the vertical direction because of the side walls of the vessel.

All these predictions concern only the final maximal displacement of the bubbles, in relation with the experimental setup and conditions. One can finally also try to relate the time variation of the foam liquid fraction $\varepsilon(t)$ to the bubble dynamics $L(t)$. Knowing the latter, it is straightforward to obtain the time evolution of the mean liquid fraction above one marker, $\varepsilon_m(t, z')$, initially located at z'. From the liquid volume conservation equation, one can write:

$$\varepsilon_m(t, z')/\varepsilon_0 = \frac{1}{1 - L(t)/h_0}\left(1 - \frac{L(t)}{L_f(z')}\right) \approx \left(1 - \frac{L(t)}{L_f(z')}\right). \tag{4}$$

The above approximation is valid for $L(t)/h_0 \ll 1$, which is the case in our experiment as $L(t) < L_{int} \ll h_0$. Alternatively, one can also infer the bubble motion (starting from different z') from the conductance $C(t)$ all over the foam height. A foam sample covering N electrodes can be cut in N small V_e volumes, which are all initially at a liquid fraction ε_0 (conductance $C(t = 0) = C_0$). At a given location z' (corresponding to the electrode i, with $i = 1$ at the foam bottom), the liquid volume conservation again implies that

$$L(t)_{z'=i} \sim (N - i)C_0 - \sum_{el=i}^{el=N} C(t). \tag{5}$$

4. Results

4.1. C_2F_6 inside and outside the foam

We performed a set of experiments with foams made of C_2F_6 gas, in contact with C_2F_6 (by previously filling the cell with that gas). Experiments were done many times for checking reproducibility, at different liquid fractions $\varepsilon_0 < 0.1$. As already stated, the goal of using C_2F_6 is to reduce the coarsening rate. With such gas and within our experimental conditions, $t_c \gg t_d$, the drainage is expected to proceed at constant bubble size. In Fig. 3a, the displacement $L(t)$ of the markers, normalized by L_{int} (final displacement of the foam–liquid interface, after complete drainage and foam collapse), is plotted for different initial vertical positions $z' = z_0/h_0$ (in this figure, for a foam at $\varepsilon_0 = 6.7\%$; similar results were found for other liquid fractions). It is found that bubbles at the foam bottom are the ones which are displaced the most—$L_f(z' = 0) = L_{int}$—and as z' increases, the final amplitude of displacement is always smaller $(L_f(z' > 0) < L_{int})$, and decreases with z'. A bubble initially located at the foam top is found not displaced. The curve for the

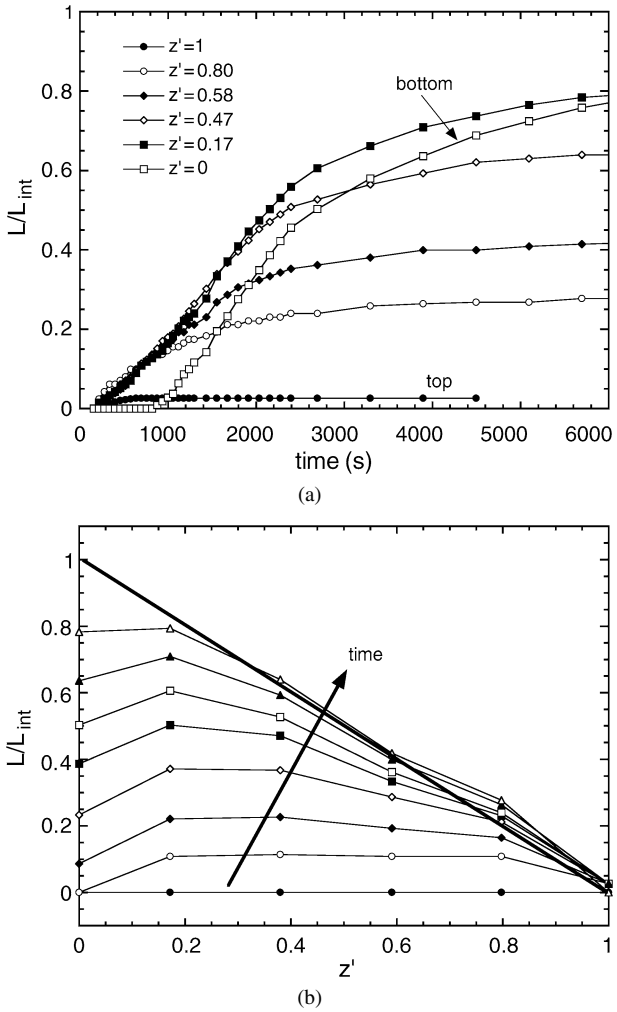

Fig. 3. Bubble displacement measurements for a C_2F_6 foam in contact with C_2F_6, during free drainage, at an initial liquid fraction $\varepsilon_0 = 6.7\%$: (a) normalized displacement vs time for different initial bubble positions z', and (b) normalized displacement vs position at different times (up to $t = 6000$ s). The solid line represents the prediction for the final maximum displacement $L_f(z')$, as discussed in Section 3.

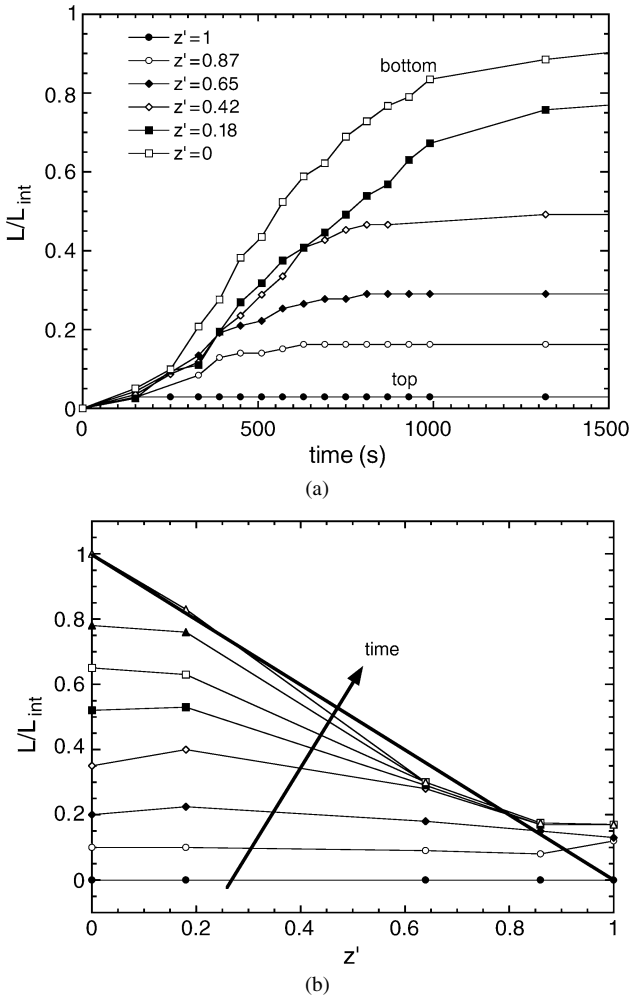

Fig. 4. Bubble displacement measurements for a N_2 foam in contact with the air, during free drainage, at $\varepsilon_0 = 7.0\%$: (a) normalized displacement vs time for different initial bubble positions z', and (b) normalized displacement vs position at different times (up to $t = 3000$ s). The solid line represents the prediction for the final maximum displacement $L_f(z')$, as discussed in Section 3.

foam bottom bubbles ($z' = 0$, thus for the foam–liquid interface) appears different from the others: it first shows a delay time before any motion is detected, and though the final L_f equilibrium value is the highest, it is reached much later than the equilibrium values at higher z'. One can also see there that for all $z' > 0$, a linear behavior with time is first found, up to a kink in the curve, always corresponding to $L/L_f(z') \approx 2/3$. Another way to present the data is to plot the same normalized displacements as a function of the initial bubble position, for different times (Fig. 3b). At large times, when the bubbles have reached their final positions, a linear dependence with z' is found. In Fig. 3b, one can also see that the dynamics are faster as z' increases (this results in non-linear curves at intermediate times): it takes less time to reach $L/L_f(z') \approx 2/3$ for z' close to 1 than for z' close to 0. For this combination of inside/outside gas, we also verified by visual observations that the bubbles diameter remains constant everywhere in the foam. So, in the case of a foam draining only without coarsening (C_2F_6 foam in contact with C_2F_6), we then draw a simple bubble-scale picture for drainage: a bubble first rises at a constant speed, then decelerates, and eventually stops.

4.2. N_2 inside and air outside the foam

We then present the results obtained for SDS foams made with N_2, in contact with air. For these foams, the bubble size is strongly changing during the drainage measurement time: the mean diameter D reaches 1 mm in 10 min. In Fig. 4a ($\varepsilon_0 = 6.2\%$), the displacement $L(t)$ of the markers (normalized by L_{int}) is plotted for different initial heights z'. As in Fig. 3a, a bubble at the foam bottom moves the most and the final amplitude of bubble displacement gets smaller with z'. Here, bubbles at the foam top are slightly displaced. At the bottom, $z' = 0$, no delay time for motion is observed, and the equilibrium value is reached as fast as for the other z'. All the curves show an inflection, indicating a maximum in the speed of the bubbles; we also found that at early times, the curves turn out to have a quadratic behavior. Other measurements, with the same gas, at liquid fractions $\varepsilon_0 < 0.1$, have given the same results. The normal-

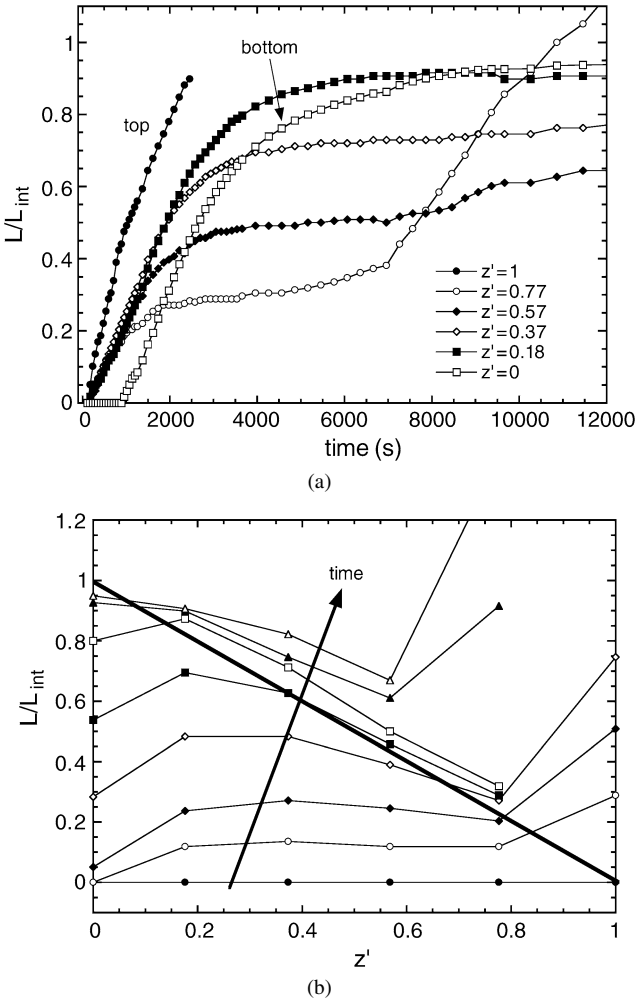

Fig. 5. Bubble displacement measurements for a C_2F_6 foam in contact with the air during free drainage, at $\varepsilon_0 = 7.4\%$: (a) normalized displacement vs time for different initial bubble positions z', and (b) normalized displacement vs position at different times (up to $t = 12{,}000$ s). The solid line represents the prediction for the final maximum displacement $L_f(z')$, as discussed in Section 3.

ized displacements as a function of the initial bubble position are shown in Fig. 4b. When bubbles are no longer moving, a linear dependence of L_f with z' is roughly found (as shown by the solid line), but not at the very top where a deviation is seen (corresponding to some local foam expansion). Finally, a major difference between the results of Figs. 3 and 4 is the timescale: for the N_2 foams, equilibrium is approached in about 1000 s, whereas for C_2F_6 more than 3000 s are typically required.

4.3. C_2F_6 inside and air outside the foam

In Fig. 5a, bubble motion measurements are now plotted, as in Fig. 3a, for a SDS foam ($\varepsilon_0 = 7.4\%$) made with the C_2F_6 gas, but now in contact with the air. When compared to the previous results, strong differences are found. First, the top of the foam sample undergoes a very large displacement, at the highest motion rate of all the markers (unfortunately $L(t)$ is no longer measurable properly after the marker has reached the top of the cell size). Inside the foam, one can see that the markers have a new behavior: after virtually stopping, they again begin to rise (at a higher rate than the initial one, and close to the one of the foam top). This new rise is quite clear for the bubble initially at $z' = 0.77$ (for $t > 6000$ s), but appears to occur also for the bubbles at $z' = 0.57$, at a later time ($t > 8000$ s). These data show that the foam volume is finally strongly increasing with time, and that this volume expansion occurs first at the foam top, and further down into the foam with time. At the bottom, as in Fig. 3a, there is a large time where no bubble motion is detected, and one can also note that the typical timescales for these foams are equal to the ones of Fig. 3a. As previously, we report in Fig. 5b the normalized displacement as a function of z'. One can see here also the large displacement of the bubble located in the top part of the foam: this displacement can even become bigger than L_{int}, and measurements are found well above the theoretical limit shown by the solid line. Complementary foam and bubble size observations show that within the bulk foam there is no coarsening as expected, but in contrast the top of the sample actually expands, just like a "soufflé." There are finally very large bubbles at the top, inducing a large and sharp vertical bubble size gradient in the foam, and with time this gradient moves downward into the foam.

Before the discussion and interpretation of these data in the following section, we can point out that by monitoring the bubble motion during foam aging, we have identified different behaviors depending on the inside/outside gases combination. Initially, a bubble can either rise at constant speed or accelerate; later, it can finally slow down and stop. However, in the case described in Section 4.3, it can resume its rising motion after even longer times.

5. Discussion

5.1. Same gas inside and outside the foam

In the following, we consider that air and nitrogen are identical, as the water solubility and diffusion constant of oxygen and nitrogen are not different enough to induce a significant change in the results: the results shown in Fig. 4 can thus be considered as those for the same gas (N_2) inside and outside, and can then be compared to those of Fig. 3 where also one gas (C_2F_6) is involved. Though the results shown in these figures share many general common features, it is clear that the nature of the gas, via its effect on the coarsening dynamics, plays a role in the bubble displacement curves. Changing the gas provides differences in the times needed for bubbles to reach their final position L_f, in the shape of the $L(t)$ curve (linear or quadratic at early times), at the foam top and bottom. As said previously, it is known that the presence or absence of coarsening during drainage modifies this drainage dynamics; here we show that accordingly it modifies the bubble motion dynamics.

So, one can now analyze in detail if these bubble upward motion observations are consistent with downward liquid flow; in other words, knowing how the liquid drains and accumulates downward ($l(t)$), in the presence or absence of simultaneous coarsening, can explain how a bubbles move upward ($L(t)$). First, the fact that for N_2 the timescale to reach final values of bubble positions is shorter than for C_2F_6 can simply be

explained by this coupling between drainage and coarsening, which strongly increases the liquid drainage rate [5,8,17,18]. As well, the bigger bubble diameter (1 mm in less than 10 min) obtained with N_2 implies that the liquid capillary hold-up at the bottom is smaller than for C_2F_6 (Eq. (3)), that the liquid velocity is faster (Eq. (2)), and thus that the condition for leakage ($\varepsilon_c = 36\%$) is obtained faster. This explains why a delay time is not observed at the foam bottom for N_2, while for C_2F_6 the slow drainage velocity makes the time to reach $\varepsilon_c = 36\%$ long enough to be macroscopically evidenced. These effects are not seen within the foam ($z' > 0$) since only at a foam–liquid interface the condition for liquid drainage ($\varepsilon_c = 36\%$) is required. Regarding the shape of the $L(t)$ curves, the linear and quadratic behaviors are also in agreement with liquid flow properties: at a given z', the bubbles move upward on the same way as the liquid accumulates below this position. For instance, for the N_2 foams, due to strong coarsening [8,17] the height of drained liquid $l(t)$ has an initial quadratic dependence with time [8,17], and this is what is also found for the bubble motion $L(t)$. Concerning the observation that the time to reach the end of the linear or quadratic part of the $L(t)$ curves (experimentally corresponding to $L/L_f(z') \approx 2/3$) decreases with z', it is also in agreement with liquid drainage and Eq. (1), stating that t_d scales with the foam height. As z' increases, the foam height above the marker and thus the drainage timescale t_d decrease. Note that a value of $L/L_f(z') \approx 2/3$ is a signature of a strong coupling between bulk and surface flow (Section 3). With C_2F_6, the final positions of the markers—$L_f/L_{int}(z')$—agree with the theoretical curve (solid line in Fig. 3b, to be compared to the dotted line in Fig. 2), confirming that the total motion of the bubbles is due to liquid drainage. For N_2, the agreement with the theoretical curve is also good, though a small expansion is seen at the top. As discussed in Section 3, coarsening cannot provide bubble motion over centimeters, but could slightly expand the foam volume, due to the decrease of the average Laplace pressure (in the case where the gas leaks towards the outside are still small). This could explain our observations: in our setup, only a small foam volume and number of bubbles are in contact with the outside, so that gas losses are probably small.

Lastly, we can compare the electrical conductivity and bubble motion measurements, within the framework of Eqs. (4) and (5). For the following comparisons, we will focus on the simplest case: C_2F_6 inside and outside the foam, meaning drainage without coarsening. The results of the conductance measurements, at four fixed heights in the foam (corresponding to z' spanning between 0.25 and 0.75) are shown in Fig. 6a, where the normalized liquid fraction $\varepsilon(t)/\varepsilon_0$ is plotted ($\varepsilon_0 = 0.06$). At long times a typical power law variation is observed, with an exponent close to -2, indicating a strong coupling between surface and bulk flow (Section 3), as already seen for such small bubbles [8,11]. Note that it is also in agreement with the value $L/L_f(z') \approx 2/3$ discussed previously. For comparison, we have plotted in Fig. 6b the time variation of $\varepsilon_m(t)/\varepsilon_0$ at different z' (from 0.18 to 0.8) extracted from the bubble motion (Eq. (4)). A power law behavior is also found at large times with an exponent equal to -2. We have thus recovered the same drainage features either by following how the

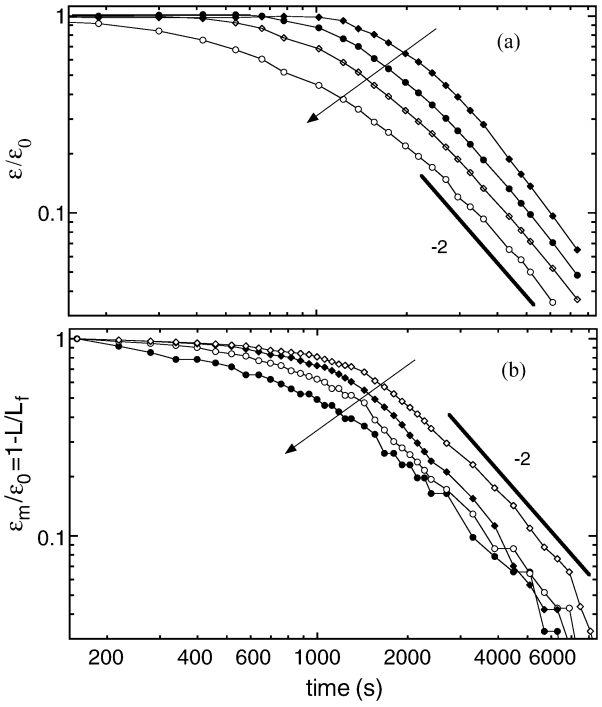

Fig. 6. (a) Normalized liquid fraction measurements as a function of time, at four different fixed positions z' (equally spaced between $z' = 0.25$ and $z' = 0.75$), for a C_2F_6 foam in contact with C_2F_6 ($\varepsilon_0 = 6\%$). (b) Time evolution of the mean liquid fraction $\varepsilon_m/\varepsilon_0$, following Eq. (4), for four initial positions z' (from $z' = 0.2$ to 0.8), deduced from bubble displacement data. The arrows indicate the direction of increase of z'. The thick solid lines, with the -2 label, represent the t^{-2} behavior discussed in Section 3.

liquid drains locally (electrical conductivity measurements) or by this method measuring how bubbles rise upwards. The good agreement, even quantitatively as it can be seen in Fig. 6, between the two methods again confirms that bubble motion is primarily driven by liquid flow downwards.

With this bubble motion tracking method, note that one cannot obtain exactly the same quantity as with the conductivity measurements (the local liquid fraction coming from a single elementary volume V_e around a position z'); however, one gets the mean value of the liquid fractions coming from all the V_e above z'. As for all these V_e, the same power law exponent is found (-2 is found at any heights, Fig. 6a) the time dependence of their mean value ε_m or of a single one are identical. Moreover, at the time where the scaling behavior occurs at a given z', it appears in fact that only a small number of V_e above z' still contain some liquid (for any $z'' > z'$, $L(t)$ has already reached its final value $L_f(z'')$). So even if $\varepsilon_m(z')$, as plotted in Fig. 6b, corresponds to the average liquid fraction above z', it is indeed probably very close to the liquid fraction in a small volume just around z', precisely as what is measured by the conductivity. Here we have demonstrated that optical measurements of bubble motion turned out to be a simple method for measuring the drainage rates, and determining the drainage regime type.

In Fig. 7, we show the time dependence of bubble positions calculated using Eq. (5) and the conductivity data; curves are calculated for seven values of z' (meaning seven reference electrodes) corresponding to $0.15 < z' < 0.95$ and are normalized

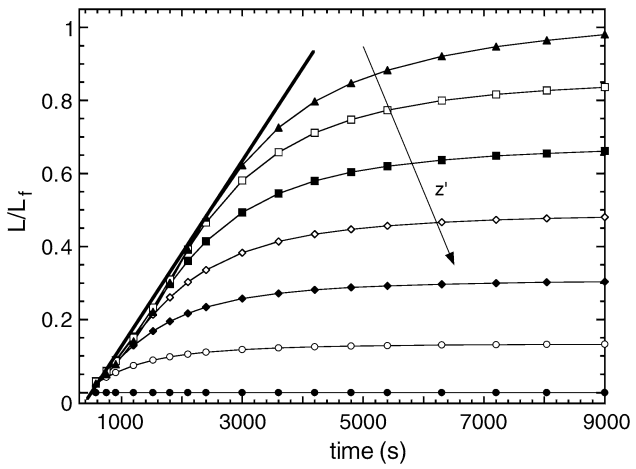

Fig. 7. Bubble displacement curves, reconstructed from the conductivity measurements ($\varepsilon_0 = 6\%$), as a function of time for different initial heights (corresponding to $0.15 < z' < 0.95$), following Eq. (5). The arrow indicates the direction of increase of z'. The solid line shows the linear behavior found at short times.

by the value L_f obtained at equilibrium time t_f for $z' = 0.15$. Here again the consistency of our different methods of measurements is verified, as we recovered a graph quite similar to the one in Fig. 3a (with an initial linear behavior, shown by the solid line). Note that this procedure does not take into account electrodes for $z' < 0.15$, close to the bottom, where the capillary hold-up is not negligible, and so it does not reproduce the delay time seen in Fig. 3a at the foam bottom.

From all these tests, it appears clearly that for these C_2F_6 or N_2 foams, the upward bubble motion and the downward liquid drainage can be deduced one from the other (despite the fact that there is or no some simultaneous coarsening).

5.2. A different gas inside and outside the foam

In Fig. 5, for the case of a C_2F_6 foam in contact with the air, a volume expansion has been observed: in comparison with N_2 foams, it is clear that it cannot be simply explained by the internal foam coarsening. The only possible origin of this effect is that the more soluble air sitting above the foam penetrates and propagates downward into the foam, resulting in a curious foam and bubble growth. This is definitively confirmed by the fact that this expansion disappears when the foam is kept in contact with C_2F_6 gas (Fig. 3).

Theoretical aspects of the coarsening of foams made of mixture of gas of different solubilities in water has been discussed in [19], showing for instance that only tiny volume fraction x of a non-diffusing gas (the rest, $(1 - x)$ corresponding to the fraction of the diffusing gas) could be already effective to drastically reducing coarsening. To get these findings, it is needed to consider both the total pressure inside the bubbles and the partial pressures of each gas, as usual when dealing with gas mixtures [19,20]. For our experiments, we have a different situation: at the time of the foam formation t_0, there is no gas mixture, and only C_2F_6 in the bubbles (the C_2F_6 volume fraction is $x = 1$) in contact with a reservoir of air ($x = 0$). This means that the partial air pressure inside the foam at t_0 is 0, as well as the partial C_2F_6 pressure outside. Despite the fact that the total pressure P_{in} is higher inside the foam bubbles than on the outside at P_o (however, note that $\delta = (P_{in} - P_o)/P_o < 1\%$), the air will diffuse into the foam since its partial pressure is lower inside. During the process, the partial pressure of the air in a foam bubble is $P_{in}^{air} = (1 - x)P_{in}$; an equilibrium value will be obtained when $x = 1 - P_o/P_{in}$. As P_o/P_{in} remains always close to 1, the equilibrium value of x is such that $x \sim 10^{-2} \ll 1$. This means that the air should enter into the foam quite widely, up to the point when C_2F_6 is completely diluted in the bubbles, with only traces of this gas remaining. This difference of partial pressure explains well the strong effect seen in the experiments. Though it is not surprising, we want to point out that it appears as a paradoxical result, since naively one could think that with a gas like C_2F_6 coarsening is reduced everywhere in the foam. But the point is that, due to the contact with the air, the opposite is found at the foam periphery where the bubble coarsens even faster than with N_2. However, the diffusion is slow enough, so that, for typical experimental timescales encountered in drainage or rheology experiments, it usually affects only the foam edges. Quantitatively, from the bubble position tracking, one can determine at which times the diffusing air is detected at a given position z'. From these estimations, we have deduced D_c, the air diffusion coefficient into the foam, $D_c = 0.015 \pm 0.005$ cm^2 s^{-1}. This is of the same order as the gas diffusion coefficient in solid foams (with open walls), and a few orders of magnitude bigger than the coefficient in water. We are now investigating in more detail this gas diffusion, especially regarding the effect on the foam topology, distribution of bubble sizes and one can expect to use it to determine foam parameters like a mean thin film thickness [3,17,18]. Lastly, one must note that, apart from the air diffusion into the foam, the rest of the results of Fig. 5 are identical to those of Fig. 3, as long as the air has not reached the measurements positions; one recovers for instance the same delay effect due to capillary holdup at the bottom.

6. Conclusions

We have shown that it is possible to measure bubble motion inside a draining and coarsening foam by using floating markers. With these simple measurements, we have identified different upward bubble motion features which can all be explained by simple ideas based on mass conservation and on the knowledge of how the liquid flows down. In that sense, it turns out that it is possible to obtain, via the bubble motion, similar information on foam drainage as obtained with more complex setup (like an electrical conductimetry one). In most of the cases, the bubble motion is solely driven by the liquid flow. However, we have found here an unexpected situation: if the foam is made of a gas less soluble than the outside one, an extra coarsening can occur, making the foam expand like a "soufflé," as a response to a gradient of partial pressure of the outside gas.

Beside the usual microscopic (at the Plateau border scale) and macroscopic descriptions (considering the foam as a effective medium), we have here developed a different and comple-

mentary picture, at the bubble scale, of foam aging. The results found here also emphasize the specificity and importance of the behaviors not only at the liquid/foam interface (with the effects of the capillary holdup) but also at the foam/outside interface (with collapse or gas exchanges).

Acknowledgment

The authors thank Danone-Vitapole for financial support.

References

[1] R.K. Prud'homme, S.A. Khan, Foams, Theory, Measurements, and Applications, Surfactant Science Series, vol. 57, Dekker, New York, 1997.
[2] D. Weaire, S. Hutzler, The Physics of Foams, Clarendon Press, Oxford/New York, 1999.
[3] (a) S. Hilgenfeldt, S.A. Koehler, H.A. Stone, Phys. Rev. Lett. 86 (2001) 2685;
(b) A. van Doornum, S. Hilgenfeldt, Phys. Rev. Lett., submitted for publication.
[4] D. Weaire, S. Hutzler, G. Verbist, E.A.J. Peters, Adv. Chem. Phys. 102 (1997) 315.
[5] A. Saint-Jalmes, M.U. Vera, D.J. Durian, Eur. Phys. J. B 12 (1999) 67.
[6] S.A. Koehler, S. Hilgenfeldt, H.A. Stone, Langmuir 16 (2000) 6327.
[7] S.J. Cox, D. Weaire, S. Hutzler, J. Murphy, R. Phelan, G. Verbist, Proc. R. Soc. London A 456 (2000) 2441.
[8] A. Saint-Jalmes, D. Langevin, J. Phys. Condens. Matter 14 (2002) 9397.
[9] D. Weaire, S. Hutzler, S. Cox, N. Kern, M.A. Alonso, W. Drenckhan, J. Phys. Condens. Matter 15 (2003) S65.
[10] H.A. Stone, S.A. Koehler, S. Hilgenfeldt, M. Durand, J. Phys. Condens. Matter 15 (2003) S283.
[11] A. Saint-Jalmes, Y. Zhang, D. Langevin, Eur. Phys. J. E 15 (2004) 53.
[12] S.A. Koehler, S. Hilgenfeldt, E.R. Weeks, H.A. Stone, Phys. Rev. E 66 (2002) 040601(R).
[13] S.A. Koehler, S. Hilgenfeldt, H.A. Stone, J. Colloid Interface Sci. 276 (2004) 420 and 439.
[14] (a) O. Pitois, C. Fritz, M. Vignes-Adler, J. Colloid Interface Sci. 282 (2005) 458;
(b) O. Pitois, C. Fritz, M. Vignes-Adler, Colloids Surf. A 261 (2005) 109.
[15] M. Safouane, A. Saint-Jalmes, V. Bergeron, D. Langevin, Eur. Phys. J. E 19 (2006) 195.
[16] K. Feitosa, S. Marze, A. Saint-Jalmes, D.J. Durian, J. Phys. Condens. Matter 17 (2005) 6301.
[17] S. Hilgenfeldt, S.A. Koehler, H.A. Stone, Phys. Rev. Lett. 86 (2001) 4704.
[18] M.U. Vera, D.J. Durian, Phys. Rev. Lett. 88 (2002) 088304-1.
[19] D. Weaire, V. Pageron, Philos. Mag. Lett. 62 (1990) 417.
[20] F.G. Gandolfo, H.L. Rosano, J. Colloid Interface Sci. 194 (1997) 31.